Silo Collapse under Granular Discharge

G. Gutiérrez,[1,2] C. Colonnello,[1] P. Boltenhagen,[2,3] J. R. Darias,[1] R. Peralta-Fabi,[2,4] F. Brau,[5] and E. Clément[2]
[1]Departamento de Física, Universidad Simón Bolívar, Apartado Postal 89000, Caracas 1080-A, Venezuela
[2]PMMH, ESPCI, CNRS (UMR 7636) and Université Paris 6 & Paris 7, 75005 Paris, France
[3]Université Rennes 1, Institut de Physique de Rennes (UMR UR1-CNRS 6251), Bat. 11A, Campus de Beaulieu, F-35042 Rennes, France
[4]Departamento de Física, Facultad de Ciencias, Universidad Nacional Autónoma de México, 04510 Mexico D.F., Mexico
[5]Nonlinear Physical Chemistry Unit, Université libre de Bruxelles (ULB), CP231, 1050 Brussels, Belgium
(Received 20 July 2014; revised manuscript received 21 November 2014; published 6 January 2015)

We investigate, at a laboratory scale, the collapse of cylindrical shells of radius R and thickness t induced by a granular discharge. We measure the critical filling height for which the structure fails upon discharge. We observe that the silos sustain filling heights significantly above an estimation obtained by coupling standard shell-buckling and granular stress distribution theories. Two effects contribute to stabilize the structure: (i) below the critical filling height, a dynamical stabilization due to granular wall friction prevents the localized shell-buckling modes to grow irreversibly; (ii) above the critical filling height, collapse occurs before the downward sliding motion of the whole granular column sets in, such that only a partial friction mobilization is at play. However, we notice also that the critical filling height is reduced as the grain size d increases. The importance of grain size contribution is controlled by the ratio $d/\sqrt{Rt}$. We rationalize these antagonist effects with a novel fluid-structure theory both accounting for the actual status of granular friction at the wall and the inherent shell imperfections mediated by the grains. This theory yields new scaling predictions which are compared with the experimental results.

DOI: 10.1103/PhysRevLett.114.018001 PACS numbers: 81.05.Rm, 45.70.Mg, 46.32.+x, 46.70.De

Granular media are ubiquitous in the food industry, agriculture, pharmacy, chemistry, and construction, to name a few. This state of matter is the subject of intense research to understand its complex and diverse properties (flow, rheology, patterns, etc.) [1–5]. Cylindrical containers are frequently used to store granular material. Silo collapses resulting of faulty construction or undetected structural deterioration are particularly vicious industrial accidents [6,7]. Each year, in spite of severe regulations defining the design and the use of granular storage devices, dramatic financial and human tolls stem from unexpected structural breakdown. Failure in reducing significantly such risks points to the fundamental difficulties in accounting properly for the thin shell structural properties and the physics of granular matter altogether. There is vast engineering literature on buckling instabilities of empty shells [8–13], but thin cylindrical shells filled with grains constitute a more complex physical system that is largely unresolved [14] and its investigation leads to open problems of great practical and scientific interest [15,16].

A common failure mode in cylindrical metal silos is the buckling under axial compression that is often triggered by gravity driven discharges of granular material [14]. Here we propose a systematic study of this problem based on laboratory scale silos. The conditions under which such silos collapse during discharge are investigated as a function of various parameters characterizing both the silo and the grains. This study is supported by a theoretical approach that couples, in the simplest possible way, the theory of buckling of thin shells and the presence of a granular material on the inside, as a source of possible imperfections.

The experimental setup is simple in its principle. A thin paper cylindrical shell is filled with granular material of size d and density ρ up to a certain height L. The silo is then emptied through a bottom circular aperture of diameter $a = 2.50 \pm 0.05$ cm which is closed with a plug during filling. The conditions of discharge are recorded by two video cameras: One recording the motion of the grains in the upper part of the silo, and a second one providing a global vision of the silo. Furthermore, we placed behind the silo two mirrors making an angle of 45° with respect to the viewing direction to provide a vision of the whole silo circumference. In these experiments, $a/d > 5$ to ensure continuous granular flow during the discharge [17,18]. Silos of different radii R, and thickness t, are prepared using a paper sheet wrapped around a metal tube and glued along a narrow band to form a cylindrical shell. The ratio R/t investigated is compatible with some industrial steel silos, for which $300 < R/t < 3000$ [15]; however, we kept the grain size much larger than the wall thickness $d \gg t$. Since paper is an anisotropic material, the silos were prepared using the same orientation of the sheet of paper and the cylindrical axis. The shell, which is inserted into a rigid cylindrical base, is fixed at the bottom and left free at the top. The preparation protocol is strict, to avoid any residual twist that would affect the shell mechanical strength. The paper Young modulus in the silo

vertical direction has been measured by flexural tests ($E = 2 \pm 1$ GPa). Figures 1(a)–1(b) show a picture and a schematic diagram of the experimental setup used to determine the collapse height L_c under grain discharge.

Most experiments were performed using spherical beads with a diameter larger than 1 mm to reduce the relative importance of disturbances, such as humidity or electrostatic interactions, with respect to gravity forces. The height L of the granular column is gradually increased after each successive full discharge until the silo collapses for $L = L_c$ during the final discharge. Figures 1(c)–1(f) show four successive snapshots of a silo after the discharge onset, for $L > L_c$, such that a collapse occurs. We observe how initial diamond shaped deformations localized near the silo bottom [Fig. 1(d)] assemble into a cluster propagating upwards on the cylindrical surface [Fig. 1(e)] until a large plastic deformation develops followed by a collapse of the silo [Fig. 1(f)] (see also movie in the Supplemental Material).

Figure 2(a) displays the position of the upper layer of grains z, as a function of time and measured relatively to the collapse height L_c, during two identical experiments where L is either below or above L_c. For $L < L_c$, localized diamond dimples may appear at the discharge onset, as shown by the dashed arrow in Fig. 2(d), but they are progressively smoothed out during the discharge such that the empty silo recovers its initial state. Two examples of this "dynamical stabilization" process are shown in the movie in the Supplemental Material [19]. For $L > L_c$, irreversible plastic deformations of the silo occur before the end of the discharge process and the onset of collapse never occurs after the downwards sliding of the whole grain column (see Ref. [37] for a systematic study of this effect).

A perfect elastic thin cylindrical shell of radius R and thickness t buckles under uniform axial compression when the applied stress exceeds the critical limit [8,9]

$$\sigma_c = \frac{Et}{\sqrt{3(1-\nu^2)}R}, \tag{1}$$

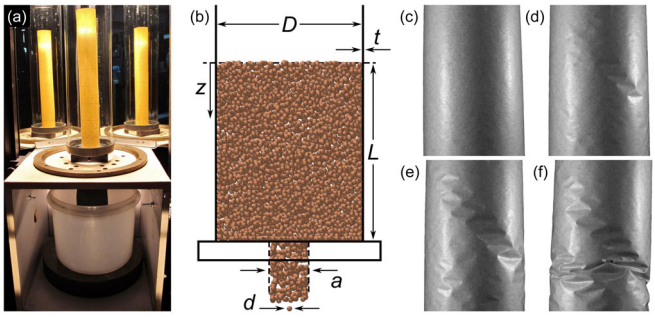

FIG. 1 (color online). Experimental setup and buckling sequence: (a) Picture of the experimental apparatus showing a paper silo, and the two mirrors used for complete visualization of the discharge. (b) Schematic cross section of the silo with its dimensions. (c)–(f) Time sequence of deformations in a collapsing silo during grain discharge. Glass beads $d = 1.5 \pm 0.1$ mm, column thickness $t = 27 \pm 5$ μm, and $R = D/2 = 2.00 \pm 0.05$ cm.

where E and ν are the Young modulus and the Poisson ratio of the cylinder's isotropic elastic material. Axisymmetric or asymmetric buckling modes occur at the same critical stress. In our case, the applied load is not uniform and is due to granular material which exerts a shear force on the inner wall of the shell. This shear force F_μ pushing down the structure is given by $F_\mu(z) = 2\pi R \int_0^z \sigma_{rz}(z')dz'$ [19]. Experiments have shown that the shear stress distribution $\sigma_{rz}(z)$ at the wall of a cylindrical column is given by the so-called Janssen's stress profile with a good accuracy either in the static [38] or in the dynamic case [39]:

$$\sigma_{rz}(z) = K\mu_w\rho_g g\lambda(1 - e^{-(z/\lambda)}), \tag{2}$$

where μ_w is the grain-wall Coulomb static friction coefficient, K is an effective vertical to horizontal redirection coefficient, and $\lambda = R/2K\mu_w$ is the Janssen's screening length. ρ_g is the bulk density of the granular medium and is related to the density of the grain material ρ through the packing fraction φ ($\rho_g = \varphi\rho$); $\varphi \simeq 0.64$ for random close packed spheres [40]. When all the contact shear forces at the wall are polarized upwards, the screening length λ is of the order of the column diameter $2R$ [38]. However, in general, just after pouring the grains, the mobilization status of the contact friction forces at the wall may depend on complicated dynamical processes, involving the pouring history [38]. The saturation of the stress profile thus takes place over a larger distance from the top surface. Some models tentatively assume a random mobilization of the friction forces at the wall to describe this effect [41]. In a simplified Janssen's picture this would be equivalent to a large value of the screening length λ, meaning that the wall bears less load than expected in the case of a full friction mobilization. However, when the discharge begins, the upward friction

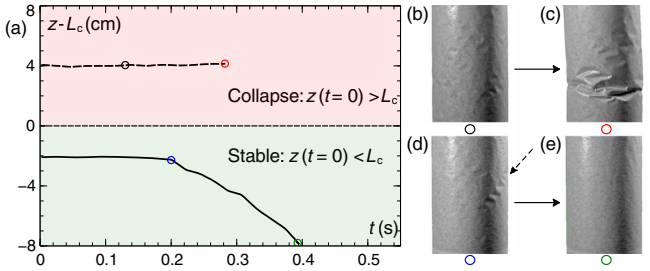

FIG. 2 (color online). Experiments where silos of radius $R = 2.00 \pm 0.05$ cm and $t = 27 \pm 5$ μm are filled by glass beads with $d = 3.0 \pm 0.1$ mm. (a) Position of the upper layer of grains z as a function of time measured relatively to the collapse height, L_c [$L = z(t = 0)$]. When $L > L_c$, irreversible deformations occur leading to a collapse of the silo. The circles indicate the time at which pictures (b)–(e) are taken. (b)–(c) Pictures of two states occurring during discharge onset for $L > L_c$. Panel (c) shows a collapsed silo. (d)–(e) Pictures of two states occurring at the discharge onset and once the discharge is completed for $L < L_c$. The solid arrows indicate the temporal evolution and the dashed arrow shows localized diamond dimples smoothed out during the discharge.

mobilization increases until the grains may move downwards. Janssen's profile can be recovered with great accuracy provided a large amount of granular material is released during the discharge [38,42]. In our experiments, we do not expect a full friction mobilization after pouring and collapse occurs at the discharge onset. Consequently, to model, in the simplest way, the fact that the upward friction polarization at the wall may not be achieved when the collapse occurs, we introduce an empirical dimensionless parameter ξ such that $\lambda = \xi R$, where ξ can be varied from $\xi = O(1)$ (full mobilization) to $\xi \gg L/R$ (random mobilization).

The stability against axisymmetric buckling of a perfect elastic thin cylindrical shell subject to the shear force F_μ induced by granular material has been studied in detail in [19]. However, in the limit $t \ll R$, the relevant scaling can simply be obtained by balancing the critical stress (1) and the applied load $[F_\mu(L) = 2\pi R t \sigma_c]$. In the case of full friction mobilization, the shear force F_μ evolves essentially linearly with z (except for $z \ll R$), whereas for random friction mobilization, it behaves as a quadratic function of z. The random mobilization regime can thus be viewed as a pseudohydrostatic regime, i.e., a hydrostatic regime with $\mu_w > 0$. Both regimes yield quite distinct scaling:

$$F_\mu(z) \simeq \pi R^2 \rho_g g z, \qquad \xi \lesssim 1 \Rightarrow L_c \simeq \frac{Et^2}{\rho_g g R^2}, \tag{3a}$$

$$F_\mu(z) \simeq \frac{\pi R \rho_g g}{2\xi} z^2, \qquad \xi \gg \frac{L}{R} \Rightarrow L_c \simeq \sqrt{\frac{Et^2}{\rho_g g R}}. \tag{3b}$$

However, even in regimes where the Taylor expansion (3a) of F_μ is not justified, the shear force can still be approximated to a good accuracy by a quadratic function for $z \in [0, \sim 1.6\xi]$ [19]. Consequently, while a pseudohydrostatic regime takes place strictly only for $L/R \ll \xi$, an effective pseudohydrostatic regime applies for L/R as large as $\sim 1.6\xi$ and leads in good approximation to the scaling (3a).

Figures 3(a)–3(d) show a parametric study of the collapse heights L_c for various grain parameters (ρ and d) and silo parameters (R and t). Figures 3(a)–3(b) clearly indicate that $L_c \sim t/\rho^{1/2}$, which is only compatible with the scaling (3a). The scaling with R reported in Fig. 3(c) is also incompatible with (3b) and it is consistent with Eq. (3a) [and improved by Eq. (8)]; this supports the contention that full mobilization is not occurring. We recall that the sliding of the granular material produces an increase of the upward friction mobilization and a classical Janssen's stress distribution at the wall should be obtained. The parameter ξ, describing the friction mobilization, should thus vary from large to $O(1)$ values. The various scalings reported in Figs. 3(a)–3(c) indicate that, even if ξ may decrease during this process, it never reaches values of order 1. These results confirm recent measurements proving that the discharge of a large amount of granular material is necessary to reach $\xi \sim 1$ [42], whereas the collapse of our silos occurs at the discharge onset (see Fig. 2).

Figure 3(d) shows that L_c depends also on the grain size d which is not a parameter of the model so far because the granular mater is assumed to be continuous in the derivation of the shear stress, Eq. (2), in agreement with experiments for $d/2R \lesssim 0.1$ [43,44]. Therefore, neither the grain size nor the rigidity of the cylinder affect the stress distribution in the regimes considered here [43,44]. One must then search for another explanation for the dependence of L_c on d. In the regime $d \gg t$ we consider, the silo wall is slightly deformed once it is filled with the grains. The shell is thus not a perfect cylinder at the discharge

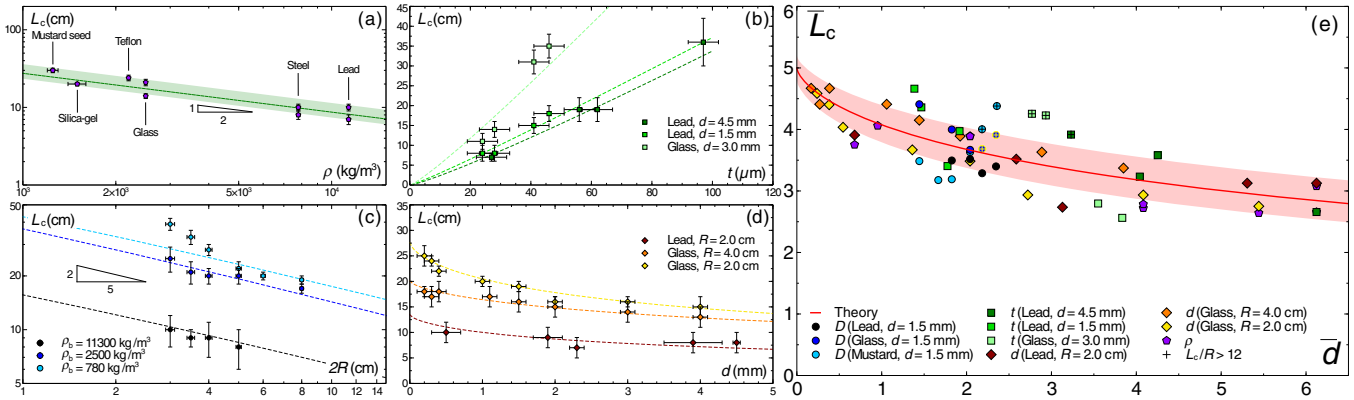

FIG. 3 (color online). Parametric exploration of the collapse height L_c and theoretical outcome. (a) L_c as a function of the grain density ρ with $t = 27 \pm 5$ μm, $R = 2.00 \pm 0.05$ cm and $d \in [0.5, 4.5]$ mm. The dashed line is obtained with Eq. (8) and the shaded area represents the region spanned by varying d in the experimental range. (b) L_c as a function of the silo thickness t (Lead, $d = 4.5 \pm 0.1$ mm, $R = 2.00 \pm 0.05$ cm/Lead, $d = 1.5 \pm 0.1$ mm, $R = 2.55 \pm 0.05$ cm/Glass, $d = 3.0 \pm 0.1$ mm, $R = 2.55 \pm 0.05$ cm). (c) L_c as a function of the silo radius R with $t = 27 \pm 5$ μm and $d = 1.5 \pm 0.1$ mm (Lead/Glass/Mustard seed). (d) L_c as a function of the grain size d with $t = 27 \pm 5$ μm (Glass, $R = 2.00 \pm 0.05$ cm/Glass, $R = 4.00 \pm 0.05$ cm/Lead, $R = 2.00 \pm 0.05$ cm). (b)–(d) The dashed lines are obtained with Eq. (8). (e) Rescaled collapse height $\bar{L}_c$ defined in Eq. (8) as a function of the rescaled grain size $\bar{d}$ defined in Eq. (7). The solid line is obtained with Eq. (8) and the shaded area corresponds to the region spanned when χ and γ are varied ($\chi = 5.0 \pm 0.2$ and $\gamma = 0.11 \pm 0.03$).

onset. We propose to describe these imperfections as geometric imperfections even if they are not necessarily stress free. An asymptotic formula, valid for small magnitude of the imperfections, has been developed in Ref. [45] to describe axisymmetric geometric imperfections and was tested in Ref. [46]. If an initial localized axisymmetric imperfection ω_0 is present on the surface of a cylindrical shell of constant thickness t, the stress σ, for which the shell buckles under axial compression, is a solution of

$$(1-\sigma/\sigma_c)^{3/2} = \eta(\sigma/\sigma_c), \tag{4}$$

where σ_c is the classical buckling stress, Eq. (1). The expression for η is determined by the shape of the imperfection as follows:

$$\eta = \frac{3^{\frac{3}{2}}|\Delta|}{2}, \qquad \Delta = \sqrt{\frac{1-\nu^2}{2}}\int_{-\infty}^{\infty}\frac{w_0(\tilde{x})}{h}e^{i\tilde{x}}d\tilde{x}, \tag{5}$$

with $\tilde{x} = \pi x/\lambda_c$ and $\lambda_c = \pi\sqrt{Rt}/[12(1-\nu^2)]^{1/4}$ (the half wavelength of the classical axisymmetric buckling mode). Equation (4) admits a simple accurate approximate solution for small Δ, where this asymptotic formula applies [19]:

$$\sigma \simeq \sigma_c(1+|\Delta|^{2/3})^{-2}. \tag{6}$$

Let us consider a localized imperfection $\omega_0 = \delta f(x)$ with $f(0) = 1$, $|f(x)| \leq 1$ and where $f(x)$ is vanishing for $|x| > \lambda_d$. At the first order in $\pi\lambda_d/\lambda_c$ we obtain [19]: $\Delta = \pi\sqrt{2(1-\nu^2)}(\delta\lambda_d/t\lambda_c)$. Assuming that the amplitude of the imperfection is of order of the thickness t and that its spatial extension is of order of the grain size d, we obtain

$$\Delta = \gamma\frac{d}{\sqrt{Rt}} = \gamma\bar{d}, \tag{7}$$

where γ is a constant fixed by the experimental data. Balancing the modified critical stress Eq. (6) with the applied load $F_\mu(L_c)$ given by Eq. (3a) and using Eq. (7) we get the collapse height

$$\bar{L}_c = \frac{\chi}{1+(\gamma\bar{d})^{\frac{2}{3}}}, \qquad \text{with} \qquad \bar{L}_c = \frac{L_c}{t}\sqrt{\frac{\rho g R}{E}} \tag{8}$$

and where $\chi = \sqrt{2\xi/\varphi}(1-\nu^2)^{-1/4}$ [19]. Comparison of this relation (dashed lines) with the data presented in Figs. 3(a)–3(d) shows a good agreement provided $\chi = 5.0 \pm 0.2$ and $\gamma = 0.11 \pm 0.03$. Notice that the grain-wall friction coefficient μ_w, the grain-grain friction coefficient μ_g, and ξ are related by $\mu_g = (2\mu_w\xi - 1)/2\sqrt{2\mu_w\xi}$ [19]. From the range of possible values for ξ, we find $\mu_g \simeq 0.60 \pm 0.06$ for $\mu_w \simeq 0.2$ which is quite reasonable.

The data reported in Fig. 3(b) indicate, by simple linear extrapolation, that the collapse height vanishes for an "apparent" finite thickness $t_c \simeq 10$ μm. This value is about 2 orders of magnitude larger than the thickness at which the silos would collapse under their own weight. Actually, the expression (8) of L_c is a convex function of t. This apparent critical thickness t_c can be obtained from the model by extrapolating the asymptote of Eq. (8) down to a vanishing L_c. Focusing on the dependence on t, Eq. (8) can be written as follows together with its asymptotic expansion

$$L_c = \frac{pt}{[1+(\frac{q}{t})^{\frac{1}{3}}]} \underset{t\gg q}{\simeq} p(t^{\frac{2}{3}} + q^{\frac{2}{3}})(t^{\frac{1}{3}} - q^{\frac{1}{3}}), \tag{9}$$

where $q = (\gamma d)^2/R$. The asymptotic expansion vanishes for $t = q$, which corresponds to the apparent critical thickness $t_c = (\gamma d)^2/R$. With the parameters used in the experiments reported in Fig. 3(b), one finds 1 μm $< t_c <$ 12 μm in good agreement with the value found by extrapolating the experimental data.

Finally, the data have been rescaled according to the scaling obtained in the model and gathered in Fig. 3(e). We observed a nice collapse of the data and a good agreement with Eq. (8). As mentioned above, a pseudohydrostatic regime is expected to apply for $L_c/R \lesssim 1.6\xi \simeq 12$. Data which do not satisfy this inequality are marked by a cross in Fig. 3(e).

In summary, we present an experimental study of granular discharge out of a thin cylindrical shell revealing paradoxical effects. The specific nature of granular matter displays contradictory stabilizing or destabilizing features controlling the structural collapse. On one hand, granular wall friction is stabilizing the structure and the columns can be filled up to levels significantly higher than what would be expected from elementary mechanical arguments. The reason is twofold: (i) pouring processes reduce the shear stress at the walls due to a lack of friction mobilization, (ii) after the discharge onset, when wall friction is fully mobilized, the localized buckling structures do not grow up to collapse because of a dynamical stabilization induced by the granular flow. Therefore, the collapse is due to the possibilities for buckling patterns to grow unbounded in the static phase prior to a full friction mobilization at the wall. On the other hand, the finite size nature of the grains creates inherent noisy patterns impinging the shell stability. To account for the filling height above which collapse is observed, we presented a theoretical analysis accounting for the lack of initial friction mobilization at the wall and granular born defects in the shell. This leads to an original scaling behavior involving all the essential mechanical and geometrical parameters and to a good quantitative agreement with the experimental outcomes. The complex "fluid"-structure problem studied here was addressed by explicit analytical methods using a minimal model which captures the essential physics associated with granular matter. The formalism could be extended to other wall geometries or shell structures. We show that such a fluid or structure problem is not only driven by forces applied during the flow but that it can also be influenced by unavoidable deformations occurring before any flow takes place. More generally, our results can have implications to other fluid or structure problems involving, for example,

advanced drilling techniques [47], plant root growth in sandy soils [48], mobility of living organisms in sand [49], and, finally, the emergent field of "soft robotics" [50], which uses the interplay between granular matter and elastic membranes to perform various tasks.

We thank L. I. Reyes, I. J. Sánchez, B. Roman, and J. E. Wesfreid for useful discussions. We thank the PCP cooperation program, CNRS and Fonacit for their support. R. P.-F. enjoyed a Sabbatical Fellowship from the Direccion General de Asuntos del Personal Academico-UNAM, and the hospitality at the PMMH (ESPCI). F. B. thanks Programme de Développement d'Expériences scientifiques (PRODEX) for financial support. This work is funded by the Agence Nationale de la Recherche (ANR) JamVibe and a Centre National d'Etudes Spatiales (CNES) grant.

[1] H. M. Jaeger, S. R. Nagel, and R. P. Behringer, Rev. Mod. Phys. **68**, 1259 (1996).
[2] P. G. de Gennes, Physica (Amsterdam) **261A**, 267 (1998).
[3] C. S. Campbell, Powder Technol. **162**, 208 (2006).
[4] I. Aranson and L. Tsimring, *Granular Patterns* (Oxford University Press, New York, 2009).
[5] B. Andreotti, Y. Forterre, and O. Pouliquen, *Granular Media: Between Fluid and Solid* (Cambridge University Press, Cambridge, England, 2013).
[6] A. Dogangun, Z. Karaca, A. Durmus, and H. Sezen, Journal of performance of constructed facilities **23**, 65 (2009).
[7] A. B. Dutta, Global J. Res. Anal. **2**, 41 (2013).
[8] S. P. Timoshenko and J. M. Gere. *Theory of Elastic Stability*, 2nd ed. (McGraw-Hill, New York, 1961).
[9] N. Yamaki, *Elastic Stability of Circular Cylindrical Shells* (North-Holland, Amsterdam, 1984).
[10] J. G. Teng, Appl. Mech. Rev. **49**, 263 (1996).
[11] J. Singer, J. Arbocz, and T. Weller, *Buckling Experiments, Experimental Methods in Buckling of Thin-Walled Structures*, Vol. 1 (Wiley, New York, 1997).
[12] J. Singer, J. Arbocz, and T. Weller, *Buckling Experiments, Experimental Methods in Buckling of Thin-Walled Structures*, Vol. 2 (Wiley, New York, 2002).
[13] *Buckling of Thin Metal Shells*, edited by J. G. Teng and J. M. Rotter (CRC Press, Boca Raton, 2003).
[14] J. M. Rotter, in *Proceedings of the International Association for Shell and Spatial Structures (IASS) Symposium 2009, Valencia*, edited by A. Domingo and C. Lazaro (Universitat Politècnica de València, Valencia, 2009).
[15] *Silos: Fundamentals of Theory, Behaviour and Design*, edited by C. J. Brown and J. Nielsen (CRC Press, Boca Raton, 1998).
[16] *Structures and Granular Solids: From Scientific Principles to Engineering Application*, edited by J.-F. Chen, J. Y. Ooi, and J. G. Teng (CRC Press, Boca Raton, 2008).
[17] I. Zuriguel, L. A. Pugnaloni, A. Garcimartín, and D. Maza, Phys. Rev. E **68**, 030301(R) (2003).
[18] C. Mankoc, A. Janda, R. Arévalo, J. M. Pastor, I. Zuriguel, A. Garcimartín, and D. Maza, Granular Matter **9**, 407 (2007).
[19] See Supplemental Material at http://link.aps.org/supplemental/10.1103/PhysRevLett.114.018001, which includes Refs. [20–36], for Detailed computation of the buckling threshold of a perfect or an imperfect elastic thin cylindrical shell subject to a shear force induced by granular material.
[20] H. A. Janssen, Zeitschrift des Vereins Deutscher Ingenieure **39**, 1045 (1895) [M. Sperl, Granular Matter **8**, 59 (2006)].
[21] G. D. Scott, Nature (London) **188**, 908 (1960).
[22] G. D. Scott, Nature (London) **194**, 956 (1962).
[23] J. D. Bernal, Proc. R. Soc. A **280**, 299 (1964).
[24] R. Lorenz, Z. Ver. Deut. Ingr. **52**, 1766 (1908).
[25] S. P. Timoshenko, Z. Math. Phys. **58**, 337 (1910).
[26] R. Lorenz, Phys. Z. **13**, 241 (1911).
[27] R. V. Southwell, Phil. Trans. R. Soc. A **213**, 187 (1914).
[28] C. M. Bender and S. A. Orszag, *Advanced Mathematical Methods for Scientists and Engineers* (McGraw-Hill, New York, 1978).
[29] D. Bushnell, AIAA J. **19**, 1183 (1981).
[30] W. Flugge, Ingenieur-Archiv **3**, 463 (1932).
[31] E. E. Lundquist, NACA Tech Note, No 473 (1933).
[32] D. J. Gorman and R. M. Evan-Iwanowski, Dev. Theor. Appl. Mech. **4**, 415 (1970).
[33] N. Yamaki and S. Kodama, Rep. Inst. High Speed Mech. **25**, Tohoku Univ, 99 (1972).
[34] G. J. Simitses, D. Shaw, I. Sheinman, and J. Giri, Compos. Sci. Technol. **22**, 259 (1985).
[35] G. J. Simitses, Appl. Mech. Rev. **39**, 1517 (1986).
[36] R. M. Nedderman, *Statics and Kinematics of Granular Materials* (Cambridge University Press, Cambridge, England, 1992).
[37] C. Colonnello, L. I. Reyes, E. Clément, and G. Gutiérrez, Physica (Amsterdam) **398A**, 35 (2014).
[38] G. Ovarlez, C. Fond, and E. Clément, Phys. Rev. E **67**, 060302 (2003).
[39] Y. Bertho, F. Giorgiutti-Dauphine, and J. P. Hulin, Phys. Rev. Lett. **90**, 144301 (2003).
[40] J. L. Finney, Proc. R. Soc. A **319**, 479 (1970).
[41] O. Ditlevsen and K. Berntsen, J. Eng. Mech. **125**, 561 (1999).
[42] C. Perge, M. Alejandra Aguirre, P. Alejandra Gago, L. A. Pugnaloni, D. Le Tourneau, and J.-C. Géminard, Phys. Rev. E **85**, 021303 (2012).
[43] T. Cambau, J. Hure, and J. Marthelot, Phys. Rev. E **88**, 022204 (2013).
[44] A. Qadir, H. Guo, X. Liang, Q. Shi, and G. Sun, Eur. Phys. J. E **31**, 311 (2010).
[45] J. C. Amazigo and B. Budiansky, J. Appl. Mech. **39**, 179 (1972).
[46] J. W. Hutchinson, R. C. Tennyson, and D. B. Muggeridge, AIAA J. **9**, 48 (1971).
[47] A. Sadeghi, A. Tonazzini, L. Popova, and B. Mazzolai, PLoS ONE **9**, e90139 (2014).
[48] L. Clark, W. Whalley, and P. Barraclough, Plant and soil **255**, 93 (2003).
[49] D. I. Goldman, Rev. Mod. Phys. **86**, 943 (2014).
[50] E. Brown, N. Rodenberg, J. Amend, A. Mozeika, E. Steltz, M. R. Zakin, H. Lipson, and H. M. Jaeger, Proc. Natl. Acad. Sci. U.S.A. **107**, 18809 (2010).